Journal of Nondestructive Evaluation (2022) 41:39
https://doi.org/10.1007/s10921-022-00872-3

A Novel AC-MFL Probe Based on the Parallel Cables Magnetizing Technique

Shenghan Wang[1] · Bo Feng[1] · Jian Tang[1] · Yanting Chen[1] · Yihua Kang[1]

Received: 24 August 2021 / Accepted: 5 April 2022

Abstract
Sensor technology is the fundamental part of intelligent manufacturing. Considering the advantages of the flexible sensor, such as being light in weight and applicable to arbitrarily curvilinear surfaces, it has become a research hotspot in the past few years. The alternating current magnetic flux leakage (AC-MFL) testing method plays a crucial role in the ferromagnetic materials manufacturing industry. However, the commonly used U-shape yoke magnetizers are large in size and difficult to be implemented on various curved surfaces, which limits the application of the method. An AC-MFL detection method based on powered parallel cables (PCs) is proposed. Furthermore, a flexible AC-MFL probe with integrating magnetizer and magnetic sensors is developed. It can be implemented in a limited space and is feasible to test parts with various curved surfaces. The finite element analysis method was used to analyze the origin of the crack signal. The directionality of the probe was analyzed and verified. In order to trade off the sensitivity and the detection stability of the probe, sensors should be placed above PC. The overall width of PC should be greater than 10 mm and less than 15 mm. Finally, the sensitivity and directionality of the probe was verified by the experiments; the application example of detecting the transition zone of a drill pipe is presented.

Keywords Parallel cables · AC magnetizing technique · AC-MFL · Flexible probe

1 Introduction

As a crucial method in nondestructive testing (NDT) technology, the magnetic flux leakage (MFL) detection method is widely used in quality control of ferromagnetic materials in automobile, petroleum and nuclear industry [1–3]. As a core component of MFL testing equipment, various types of sensors and probes are developed [4–6] to meet different application demands. The alternating current magnetic flux leakage (AC-MFL) method has ascendancy in on-line inspection for cracks on the surface of the ferromagnetic parts [7]. Fujiwara et al. developed an on-line testing system for the surface crack of ferromagnetic parts based on the AC-MFL method [8]. Gotoh Yuji et al. used the AC-MFL method to distinguish adjacent defects and proposed a method that can detect outer surface cracks by the endo-probe [9, 10]. Sophian et al. studied the pulsed MFL method, which can detect and classify defects [11]. Minoru et al. proposed an AC-MFL imaging method based on the U-shape magnetic yoke and the TMR array [12]. All these research results promoted the development of the AC-MFL method.

In the existing AC-MFL techniques, parts are mostly magnetized by the U-shape yoke. However, on the one hand, the size of the yoke imposes limits on detecting the inside surface of narrow tubes. On the other hand, it is hard to contour machine the U-shape yoke, which means magnetizing curved surfaces is challenging, so the current probes are inadequate for the detection needs of various parts in the industry. Additionally, for the traditional AC-MFL probe, the magnetizer and detecting units are designed separately, and thus, it is tremendously difficult to ensure the relative position between the units and the magnetic field during the scanning movement, which may cause a lot of noise. Considering that eddy current probes are highly integrated and mostly flexible nowadays [13, 14], it is worth developing an AC-MFL probe that integrates magnetization and detection units and is applicable in various inspection environments to detect various curved parts, such as camshaft, bearing race and the transition zone of drill pipe, etc.

✉ Yihua Kang
yihuakang@hust.edu.cn

[1] State Key Lab of Digital Manufacturing Equipment and Technology, Huazhong University of Science and Technology, Wuhan, China

Published online: 23 April 2022

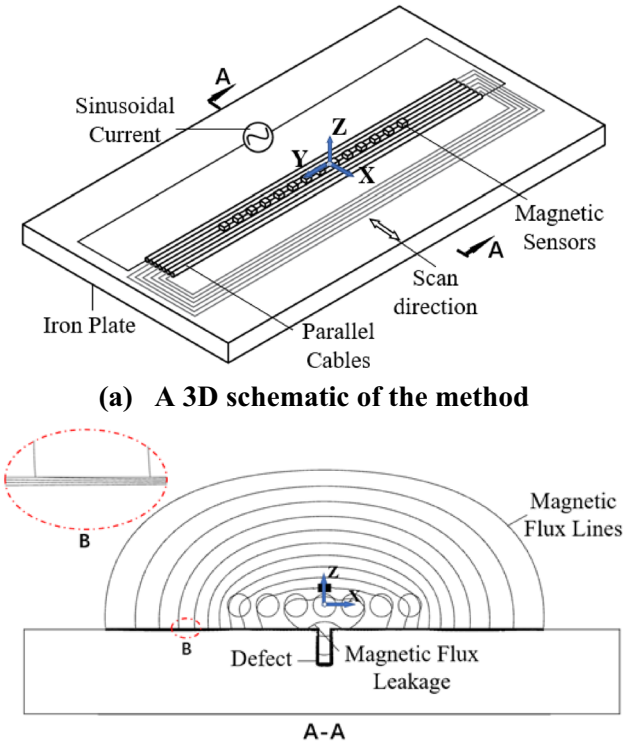

Fig. 1 The schematic of the method

This paper proposes an AC-MFL testing method based on the powered parallel cables (PCs) attaching to the surface of the workpiece for magnetization. Meanwhile, by placing magnetic sensors on the backside of the PC, a novel flexible AC-MFL probe is formed, which can test parts with an arbitrary curved surface in a limited space and complex environment. In Sect. 2, the method is described. In Sect. 3, firstly the generating mechanism of crack signal is discussed and verified by the finite element analysis model, and then the approaches to increase the magnetization field generated by the PC are proposed and analyzed. In Sect. 4, the detection capability of the probe is verified by the cylinder bearing experiment. The conclusion is given and the future work is discussed in Sect. 5.

2 Method

The detection method is illustrated in Fig. 1. In Fig. 1a, b, the overall schematic and the cross section with the enlarged fragment which exhibits the detail of flux lines are shown respectively. During testing, monolayer PC with cables connected in series keeps attaching to the surface of the part, magnetizing the part with "near-zero lift-off", and the MFL will be detected by magnetic sensors with scanning along the perpendicular direction of the current. In this method,

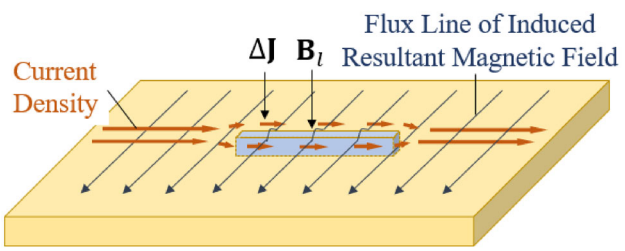

Fig. 2 Two electromagnetic field disturbances caused by a crack

to get the relatively strongest leakage field and ensure the conformability of the sensor array, the magnetic sensors are centrally arranged on the backside of cables along the axis direction of the cables. The alternating magnetic field generated by cables will gather in the skin layer of parts, so the excitation magnetic field intensity required for detection is much smaller than that of direct current MFL detection. The outstanding advantage of this method is to realize "near-zero lift-off" magnetization. On the one hand, it can reduce the loss of magnetic fields in space. On the other hand, the flexible cables attach to various surfaces with "near-zero lift-off", which can avoid the interference of different shapes of the workpiece on the magnetization.

To simplify the description, a Cartesian coordinate is built as shown in Fig. 1. The origin of the coordinate is located at the midpoint of the line of the cable centers. The X-axis is the scan direction, the Y-axis is parallel to the current direction, and the Z-axis is the lift-off direction. In the following content, the magnetic field component in the X-axis direction is taken as an example to illustrate, and the magnetic field component at the peak moment under the excitation of sinusoidal current is mainly discussed.

3 Simulation and Analysis

3.1 The Main Component of the Perturbed Magnetic Field in Ferromagnetic Parts

As shown in Fig. 2, when magnetizing parts by sinusoidal exciting current, the crack on the carbon steel plate not only generates the MFL field $\mathbf{B}_l$ in the air, but also produces the induced current density disturbance $\Delta\mathbf{J}$, which causes the secondary magnetic field disturbance $\mathbf{B}_{\Delta\mathbf{J}}$. The disturbing signal measured by sensors comes from the aforesaid two magnetic field perturbances during the scan, which can be described as

$$\Delta\mathbf{B} = \mathbf{B}_l + \mathbf{B}_{\Delta\mathbf{J}}.$$

The current density $\Delta\mathbf{J}$ drops in the air gap and rises at the edges [15], so the $\mathbf{B}_{\Delta\mathbf{J}}$ in air above the crack distributes

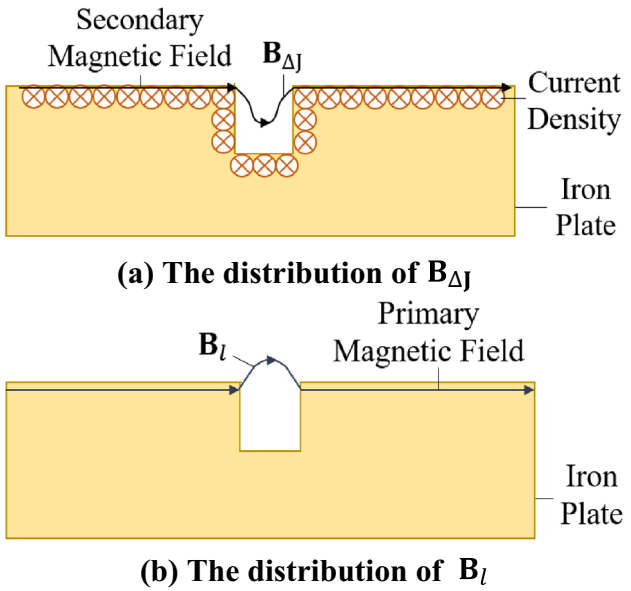

Fig. 3 The distribution of magnetic field disturbances

like the valley shape, which is high on both sides and low on the center as shown in Fig. 3a. While the distribution of $\mathbf{B}_l$ is like the peak shape, which is low on both sides and high on the center as shown in Fig. 3b.

To verify the signal source, a 2D finite element model is established by COMSOL Multiphysics as shown in Fig. 4a. The dot-dash line is the measuring path. The diameter of the cable is Ø 0.4 mm. The material is set to copper. The thickness of the insulation layer is 0.15 mm. The amplitude of the current is 0.7 A. Due to the $\mathbf{B}_{\Delta J}$ and $\mathbf{B}_l$ distribute diversely in different exciting frequency, multiple frequencies are set in the model. Furthermore, set two different materials for the examined plate as a comparison: one is aluminum plate whose conductivity is 3.70×10^7S/m and the relative permeability is 1, the other one is carbon steel plate whose conductivity is 1.12×10^7S/m and the relative permeability is 200. The magnetic flux density which has subtracted by the background magnetic field (no crack in the model) on the measuring path is denoted as $\Delta\mathbf{B}$, and the $\Delta\mathbf{B}$ distributions of aluminum and steel plate are plotted in Fig. 4b and c, respectively, where the $\Delta\mathbf{B}$ is positive in the same direction as the magnetization field, and negative in the reverse direction. In Fig. 4d, the maximal absolute values of $\Delta\mathbf{B}$ in different frequencies are plotted.

It can be seen in Fig. 4b, c that the direction of $\Delta\mathbf{B}$ is identical to the magnetizing field in the steel plate model, while the direction of $\Delta\mathbf{B}$ is opposite to the magnetizing field in the aluminum plate model. Additionally, the distribution of $\Delta\mathbf{B}$ along X-axis direction is different between the steel and aluminum plate. According to Fig. 3 and above analysis, in the frequency range from 1 to 100 kHz, the main component of $\Delta\mathbf{B}$ above the steel plate is MFL field.

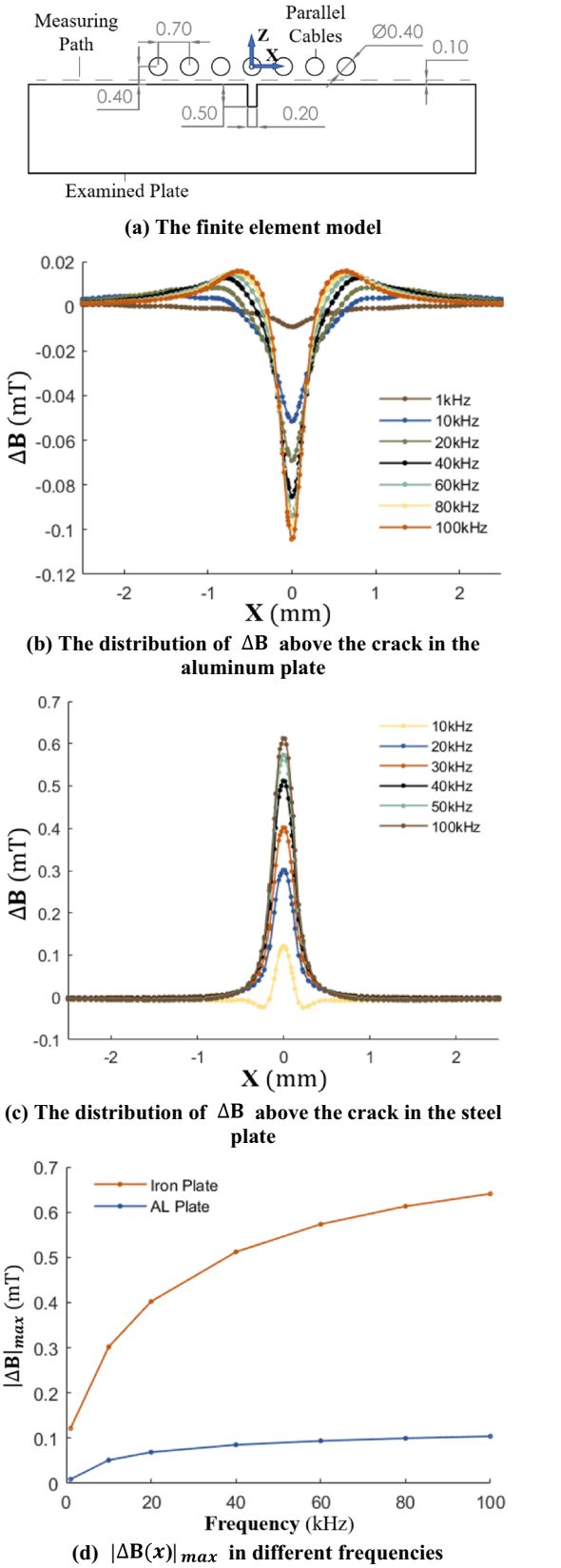

Fig. 4 The comparison simulation of disturbance magnetic field in aluminum and steel plate

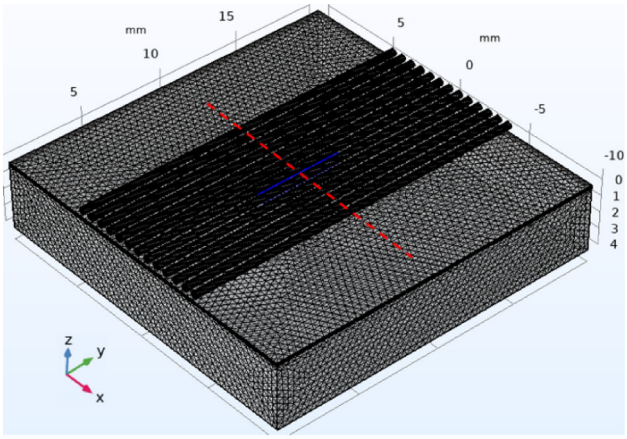

(a) The FEM model in COMSOL

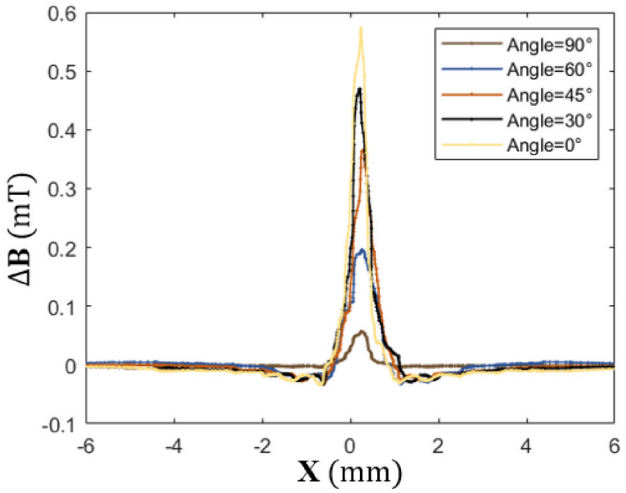

(b) The distribution of ΔB above the crack at different probe angles

Fig. 5 The simulation of different angles of the crack

Based on the result in Fig. 4d, we know that the peak value of $\Delta\mathbf{B}$ in a steel plate is larger than the value in an aluminum plate. Thus, we can conclude that for the crack parallel to the current direction, the AC-MFL detection method will get higher intensity perturbation magnetic signals. Meanwhile, in the frequency range from 1 to 100 kHz, the intensity of the leakage field is increasing as the frequency growing, which is beneficial to crack detection.

3.2 The Directionality of the Probe

The MFL signal amplitude is almost zero when the magnetic flux line is parallel to the crack [16]. While for the AC-MFL method, the induced eddy current is orthogonal to the leakage magnetic field, which may help detect cracks in the insensitive direction [17]. Thus, a 3D COMSOL model is built, as shown in Fig. 5, to help analyze the directionality of the probe. The number of cables is 13, the length, width and depth of the crack is 5 mm, 0.2 mm, 0.5 mm respectively, the amplitude and frequency of excitation current are 0.7 A and 100 kHz respectively, and the rest setting is identical to the model in Fig. 5a. Set PC angles to 0°, 30°, 45°, 60°, 90° with Y-axis in turn. The scanning path is located in the center of the workpiece, parallel to the X-axis and 0.1 mm from the upper surface of the steel plate. The magnetic flux density $\Delta\mathbf{B}$ which has subtracted by the background magnetic field is acquired as shown in Fig. 5b.

In Fig. 5b, as the angle decreases, the maximal $\Delta\mathbf{B}$ keeps increasing which is in line with the MFL test [16]. While the value of $\Delta\mathbf{B}$ is not zero when the magnetic flux line is parallel to the crack, which is identical to the orientation of the alternating current field measurement (ACFM) method. The $\Delta\mathbf{B}$ is mainly from the disturbance of the eddy current [17].

Based on the above analysis, the perturbance field $\Delta\mathbf{B}$ relates to both eddy current and leakage magnetic field. In ACFM, the main measurement direction are Y- and Z-axis directions. In AC-MFL testing, both magnetic components in X- and Z-axis directions are corresponding to cracks. To avoid confusion between ACFM and AC-MFL methods, the measuring direction of the probe is set as X-axis.

3.3 Analysis of PC Magnetizer

Consistent with the mechanism of DC MFL detection [18], in AC-MFL detection, it is very important to magnetize the detected part to saturation, but it is not an essential condition for the generation of leakage field from surface crack [19].

The intensity of the leakage field depends on the intensity of the magnetization field. For PC magnetizers, there are three ways to increase the intensity of the magnetizing field: boosting the amplitude of exciting current, adding more cables and decreasing the distance between the lower surface of cables and the surface of the workpiece, which is denoted as d_c.

The maximum current allowed in a single cable is proportional to its cross-sectional area, but on the other side, the diameter of the cable is related to the lift-off value of magnetic sensors, which should not be too large. Therefore, the upper limit of magnetizing current is restricted.

Increasing the number of cables in the X-axis direction will boost the magnetization intensity, whereas the more the number of cables, the farther the cables on both sides are from the detection area, thus the smaller the contribution will be. Due to the effect of a single cable on the magnetization field of detection area is mainly related to the relative distance, the independent value is converted from the number of cables to the total width of cables. Further analysis is based on the simulation model shown in Fig. 4a. The frequency of current is set to 100 kHz, the examined plate is replaced by a steel plate with an undamaged surface, set the value of d_c to 0 mm

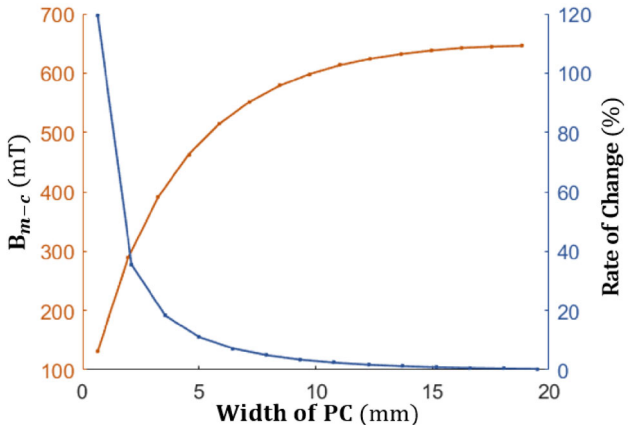

Fig. 6 The simulation result of distribution of B_{m-c} with the width of cables

and changing the number of 26 AWG cables. The relationship between the maximal absolute value of the magnetization field $\mathbf{B}_{m-c}$ and the width of PC is shown in Fig. 6.

It can be seen that the magnetization field intensity of the detection area increases with the decreasing growth rate. The rate of change drops dramatically when the width is less than 5 mm. It is less than 2% at 10 mm and close to 0 when the width is 15 mm, which means the cable is more than 7.5 mm away from the central cable has a rare effect on increasing the magnetization intensity of detection area. To trade off the probe size and magnetization intensity, the reasonable range of the width of PC is from 10 to 15 mm in the application.

The lift-off value of PC mainly depends on the positioning of magnetic sensors. To be specific, place sensors above PC, the value of d_c could go down to 0. While d_c should be related to the height of sensors, if PC is on the top. On the basis of the model shown in Fig. 4a, change d_c from 0 to 1.4 mm (the intervals are 0.1 mm from 0 to 0.4 mm and 0.2 mm from 0.4 to 1.4 mm). Measure the horizontal component of magnetic flux density $\Delta\mathbf{B}_x$ above PC at the central axis when the range of d_c is from 0 to 1.0 mm. Meanwhile, measure $\Delta\mathbf{B}_x$ below PC when d_c is from 0.4 to 1.4 mm. The results are shown on Fig. 7a and b, respectively.

From Fig. 7, the overall value of $\Delta\mathbf{B}_x$ above PC is smaller but gentler compared to the value of $\Delta\mathbf{B}_x$ under PC. For the probe, the sensitivity and stability should be trade off [20]. Thus, sensors should be placed on the top. In Fig. 7a, $\Delta\mathbf{B}_x$ tends to linear when the distance from the top of PC is over 0.4 mm. In fact, the distance mainly depends on the size of sensor, so sensor whose measuring point height is around 0.5 mm is selected and fixed above the PC to form an integrated probe. Set d_c to 0.3 mm, When the lift-off value of the probe fluctuates $\pm$ 0.1 mm, the maximum change rate of the $\Delta\mathbf{B}_x$ is about 9.8%, which is less than 10% and is adequate for engineering applications [21].

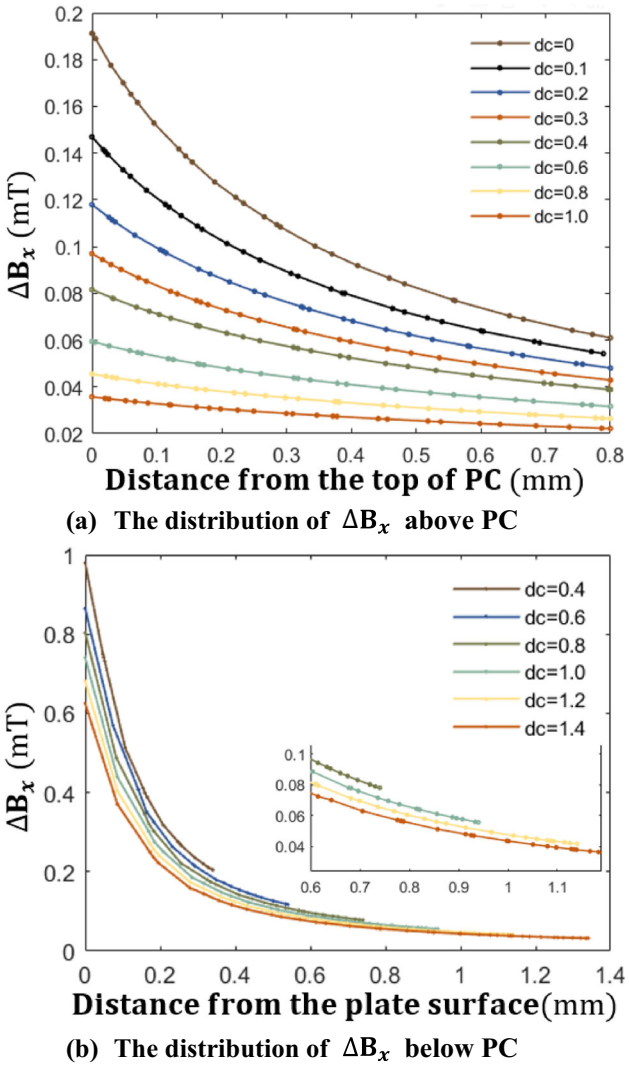

Fig. 7 The simulation result of distribution of $\Delta\mathbf{B}_x$ with the lift-off value

4 Experiments

A series of experiments are set to verify the detection capability of the probe. The testing object is a carbon steel plate with four artificial cracks machined by electrical discharge. The length of cracks is 20 mm. The width of cracks is 0.2 mm, which can meet most testing requirements in practice. The depth of cracks is 0.2 mm, 0.3 mm, 0.4 mm, 0.5 mm respectively. The PC magnetizer is composed of the 20 26 AWG cables with a total width of 14 mm and placed 0.3 mm above the plate. A TMR unit with model TMR 2001 manufactured by the MultiDimension Technology, whose sensitivity is shown on Fig. 8a and the bandwidth of $-$ 3 dB is 200 kHz, is placed on the backside of the PC, measuring the tangential magnetic field component in the X-axis direction. The experiment setup is shown in Fig. 8b. The sinusoidal signal generator supplies power to PC, the current amplitude

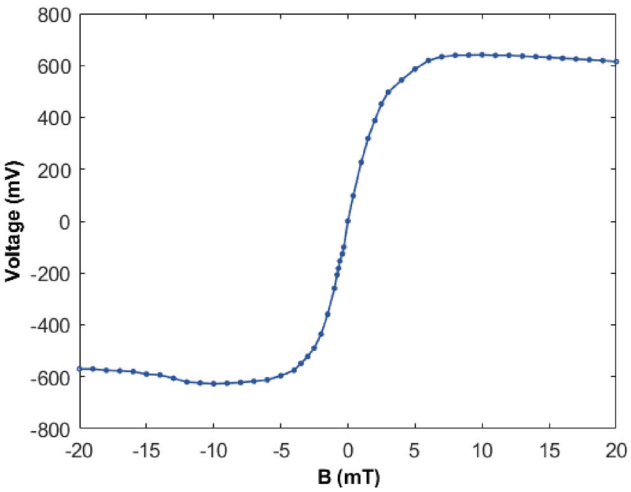

(a) The sensitivity of TMR 2001

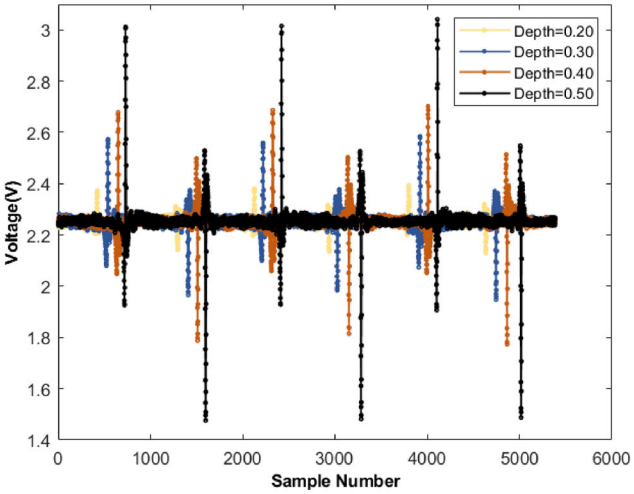

(c) The detection signal of different cracks

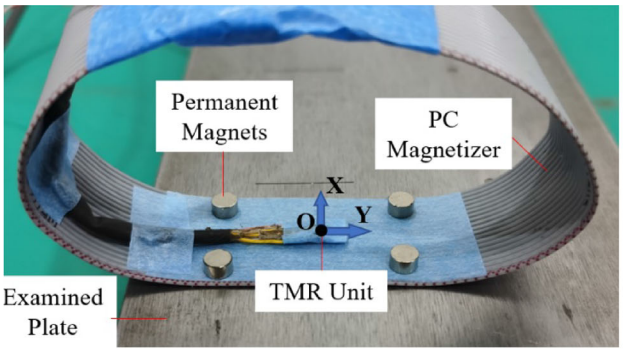

(b) The experiment setup

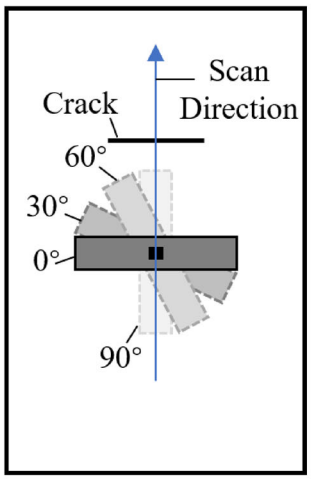

(d) The schematic diagram of scan

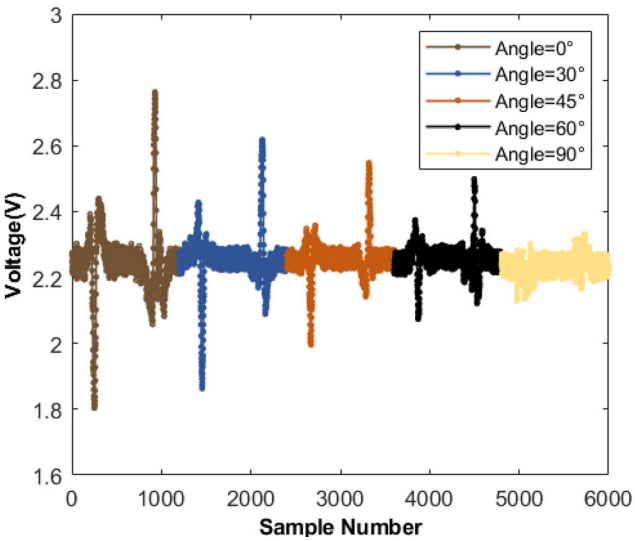

(e) The detection signals from different angles

Fig. 8 Experiments and results

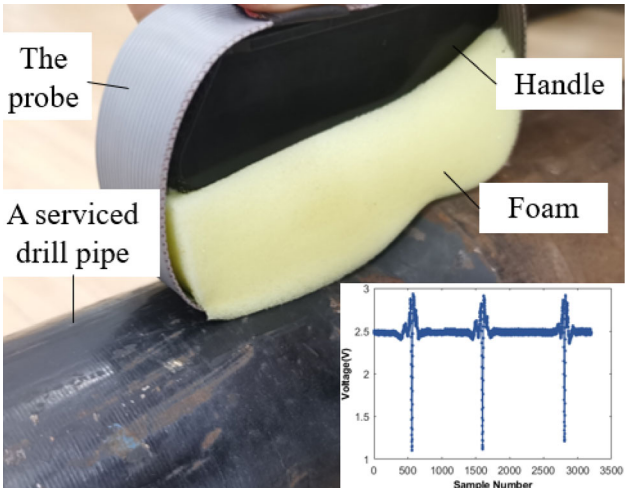

Fig. 9 The application example

is 0.7 A and the frequency is 100 kHz. The output of the TMR unit is connected to a detector circuit and an amplifier with an amplification factor of about 60 dB. The processed signal is connected to the DAQ system and then stored in and displayed on the laptop. The probe reciprocates along the X-axis. The crack signals after alignment are shown in Fig. 8c. The amplitude keeps climbing with the depth. The average SNR of each group of voltage signals is 9.80, 18.81, 21.66 and 26.58. Then scan the crack with a depth of 0.4 mm from different angles by the probe. The schematic diagram and experimental results of the scanning are shown in Fig. 8d and e, respectively.

It can be seen from Fig. 8e that the amplitude of signal attenuates with the increasing angle. When the angle is 90°, the perturbance of signal still exist. The result is in accord with the simulation result.

5 Application

The flexible probe can be used to inspect most curved surfaces. In Fig. 9, an example of testing drill pipe transition zone is shown. The foam evenly exerts pressure on the magnetic sensor and PC to make them attaching to the surface during test. An axial crack with a width of 0.5 mm and a depth of 1.0 mm was machined on the transition zone. Scan the crack for three times in one direction and the signal is shown in Fig. 9.

6 Conclusion and Future Work

In this paper, we proposed an AC-MFL detection method and a novel probe based on the "near-zero lift-off" magnetization by the powered PC. The crack signal is proven to be generated mainly by the MFL field in ferromagnetic materials. In order to ensure the stability and strength of the crack signal simultaneously, the magnetic sensor should be placed on the top of PC, the distance between the measuring point and the top of PC should be larger than 0.4 mm, the lift-off value of PC should be around 0.3 mm. The total width of PC is supposed to be greater than 10 mm and less than 15 mm. By magnetizing the part with "near-zero lift-off", the excitation current with 0.7 A amplitude is enough for detecting the crack with a width of 0.2 mm and a depth of 0.2 mm on the surface of the cylindrical surface. The probe has the highest sensitivity when it is perpendicular to the crack, but it still has disturbance signal even it is parallel to the crack.

In fact, the frequency of current has a great impact on the crack signals, which could be optimized in subsequent research. Meanwhile, in AC-MFL detection, the influence of the crack depth on the detection signal is also related to the excitation frequency, which is supposed to be studied in future work.

Acknowledgements This paper was financially supported by the National Natural Science Foundation of China (NNSFC, 51875226).

References

1. Wang, Z.D., Gu, Y., Wang, Y.S.: A review of three magnetic NDT technologies. J. Magn. Magn. Mater. **324**, 382–388 (2012)
2. Christen, R., Bergamini, A., Motavalli, M.: Influence of steel wrapping on magneto-inductive testing of the main cables of suspension bridges. NDT E Int. **42**(1), 22–27 (2009)
3. Sun, Y.H., Wu, J.B., Feng, B., Kang, Y.H.: An opening electric-MFL detector for the NDT of in-service mine hoist wire. IEEE Sens. J. **14**(6), 2042–2047 (2014)
4. Li, E.L., Kang, Y.H., Tang, J., Wu, J.B.: A new micro magnetic bridge probe in magnetic flux leakage for detecting micro-cracks. J. Nondestruct. Eval. **37**, 46 (2018)
5. Wu, D.H., Su, L.X., Wang, X.H., Liu, Z.T.: A novel non-destructive testing method by measuring the change rate of magnetic flux leakage. J. Nondestruct. Eval. **36**, 24 (2017)
6. Wu, J.B., Yang, Y., Li, E.L., et al.: A high-sensitivity MFL method for tiny cracks in bearing rings. IEEE Trans. Magn. (2018). https://doi.org/10.1109/TMAG.2018.2810199
7. Tsukada, K., Yoshioka, M., Kiwa, T., Hirano, Y.: A magnetic flux leakage method using a magnetoresistive sensor for nondestructive evaluation of spot welds. NDT E Int. **44**(1), 101–105 (2011)
8. Fujiwara, H., Sakamoto, T., Nishimine, T., et al.: Development of ac magnetic leakage flux testing system. In: International Symposium on Applied Electromagnetics and Mechanics, 2001, pp. 527–528 (2001)
9. Gotoh, Y., Takhashi, N.: Study on problems in detecting plural by alternating flux leakage testing 3-D nonlinear eddy current analysis. IEEE Trans. Magn. **39**, 1527–1530 (2003)
10. Gotoh, Y., Sakurai, K., Takahshi, N., et al.: Electromagnetic inspection method of outer side defect on small and thick steel tube using both AC and DC magnetic fields. IEEE Trans. Magn. **45**, 4467–4470 (2009)

11. Sophian, A., Tian, G.Y., Zair, S.: Pulsed magnetic flux leakage techniques for crack detection and characterization. Sens. Actuators A **125**, 186–191 (2006)
12. Hayashi, M., Kawakami, T., Saito, T., Sakai, K., Kiwa, T., Tsukada, K.: Imaging of defect signal of reinforcing steel bar at high lift-off using a magnetic sensor array by unsaturated AC magnetic flux leakage testing. IEEE Trans. Magn. (2021). https://doi.org/10.1109/TMAG.2020.3017722
13. Grimberg, R., Udpa, L., Savin, A., Steigmann, R., et al.: 2D eddy current sensor array. NDT E Int. **39**, 264–271 (2006)
14. Chen, T., He, Y., Du, J.: A high-sensitivity flexible eddy current array sensor for crack monitoring of welded structures under varying environment. Sensors **18**(6), 1780 (2018)
15. Li, W., Yuan, X.A., Chen, G.M., Yin, X.K., Ge, J.H.: A feed-through ACFM probe with sensor array for pipe string cracks inspection. NDT E Int. **67**, 17–23 (2014)
16. Wu, J.B., Sun, Y.H., Kang, Y.H., Yang, Y.: Theoretical analyses of MFL signal affected by discontinuity orientation and sensor-scanning direction. IEEE Trans. Magn. (2015). https://doi.org/10.1109/TMAG.2014.2350460
17. Wu, D.H., Liu, Z.T., Wang, X.H., Su, L.X.: Composite magnetic flux leakage detection method for pipelines using alternating magnetic field excitation. NDT E Int. **91**, 148–155 (2017)
18. Song, K., Chen, C., Kang, Y., et al.: Mechanism study of AC-MFL method using U-shape inducer. Chin. J. Sci. Instrum. **33**(9), 1980–1985 (2012)
19. Sun, Y.H., Kang, Y.H.: Magnetic mechanisms of magnetic flux leakage nondestructive testing. Appl. Phys. Lett. **103**(18), 184104 (2013)
20. Wu, D.H., Zhang, Z.Y., Liu, Z.L., Xia, X.H.: 3-D FEM simulation and analysis on the best range of lift-off values in MFL testing. J. Test. Eval. **43**, 673–680 (2015)
21. Li, W., Chen, G.M., Yin, X.K., Zhang, C.R., Liu, T.: Analysis of the lift-off effect of a U-shaped ACFM system. NDT E Int. **53**, 31–35 (2013)